Carbohydrate Polymer Technologies and Applications 2 (2021) 100028

Contents lists available at ScienceDirect

Carbohydrate Polymer Technologies and Applications

journal homepage: www.elsevier.com/locate/carpta

Co-culture fermentation on the production of bacterial cellulose nanocomposite produced by *Komagataeibacter hansenii*

Hetian Hu, Jeffrey M. Catchmark*, Ali Demirci

Department of Agricultural and Biological Engineering, 226 Agricultural Engineering Building, Pennsylvania State University, University Park, PA 16802, United States

ARTICLE INFO

Keywords:
Bacterial cellulose
Pullulan
Komagataeibacter hansenii
Aureobasidium pullulans
Co-culture
Exopolysaccharides

ABSTRACT

Bacterial cellulose (BC[1]) is a biomaterial produced by various strains of microorganisms. BC has improved strength and unique structural properties as compared to plant cellulose, thus has many usages in the food and pharmaceutical industries. In our previous study, a novel co-culture agitated fermentation of *Komagataeibacter hansenii*, a BC producer, with *Aureobasidium pullulans*, a producer of pullulan polysaccharide, had been demonstrated where the BC produced exhibited improved mechanical properties. Therefore, this study is undertaken to analyze BC production under different medium composition using response surface methodology (RSM) in shake-flasks and benchtop bioreactors. A verified local high point provided 22.4% higher BC production and 4.5- to 6- folds higher elastic moduli in shake-flasks and bioreactors compared to the baseline media. Overall, the study had revealed the potential of the co-culturing method to enhance BC production while maintaining the desired mechanical properties of BC produced in shake-flasks and larger scale bioreactors.

1. Introduction

Bacterial cellulose (BC), having a similar chemical structure as plant cellulose, is composed of glucose linked by β (1–4) glycosidic bonds. BC is produced by various species of microorganisms, such as *Komagataeibacter, Rhizobium*, and *Sarcina* (Fang & Catchmark, 2015; Ross, Mayer & Benziman, 1991). Due to its unique properties such as ultrafine reticulated crystalline structure, high tensile strength, high purity, and biocompatibility, BC has a great potential to be used for many applications (Backdahl et al., 2006; Fang & Catchmark, 2015; Hsieh, Yano, Nogi & Eichhorn, 2008). In the food industry, *nata de coco*, a traditional dessert from Philippines, is made directly from BC. BC can also be added into gel-formed foods or pastes to help retain humidity, improve texture, and enhance stickiness (Nakagaito, Iwamoto & Yano, 2005; Okiyama, Motoki & Yamanaka, 1992, 1993). In the pharmaceutical industry, BC is used as wound dressings (XCell, Medline Industries Inc., Northfield, IL), and it also has the potential to be used as a drug/antibiotic release material (Muangman, Opasanon, Suwanchot & Thangthed, 2011), organ/partial organ replacement (Nimeskern et al., 2013), and as artificial blood vessels (Klemm et al., 2016; Wippermann et al., 2009). Other applications of BC include facial masks, and other cosmetic use. (Amnuaikit, Chusuit, Raknam & Boonme, 2011; Lin et al., 2013).

For industrial production of BC, the ultimate goal is to improve the production yield and quality (especially modulus, elongation, and tensile strength) of BC. Many approaches have been studied to achieve this ultimate goal. In previous studies, a number of BC-producing strains, including type culture and newly isolated strains, had been screened, and strains with significantly better BC production have been identified in various types of media (Gullo et al., 2017; Gullo, China, Petroni, Gregorio & Giudici, 2019; Toyosaki et al., 1995). Besides strain screening, many studies had been performed to improve BC production and mechanical properties by defining and maintaining the optimum cultivation parameters like pH, temperature, and type of carbon sources (Jagannath, Kalaiselvan, Manjunatha, Raju & Bawa, 2008; Çoban & Biyik, 2011; Fang & Catchmark, 2015; Kuo, Chen, Liou & Lee, 2016). Many attempts have also been made to produce BC using low-cost fermentation wastewater or industrial byproducts (Vazquez, Foresti, Cerrutti & Galvagno, 2012; Velásquez-Riaño & Bojacá, 2017; Zhao et al., 2018). Although various types of approaches had been examined, polysaccharide addition during the BC fermentation seems to be one of the most effective ways of enhancing the BC production and mechanical properties due to the direct incorporation of polysaccharides into the BC matrix during its formation. Polysaccharides such as carboxymethyl cellulose (CMC) had been proven helpful for improving BC production for 1.7-folds (Cheng, Catchmark & Demirci, 2009a, 2011),

* Corresponding author.
E-mail addresses: jcatchmark@psu.edu, jcatchmark@engr.psu.edu (J.M. Catchmark).

[1] Uncommon abbreviation used: BC – Bacterial Cellulose

https://doi.org/10.1016/j.carpta.2020.100028
Received 22 July 2020; Received in revised form 12 December 2020; Accepted 16 December 2020

and the exopolysaccharide (EPS) produced by an *E. coli* strain lead to an 81.9% increase in Young's modulus and a 79.3% improvement in tensile strength for the BC produced with its existence (Liu & Catchmark, 2019). Linear polysaccharides such as glucomannan and xylan could also incorporate into BC matrix, altering the interconnectivity of BC microfibrils, thus shifting BC production and mechanical behaviors (Chi & Catchmark, 2017; Iwata, Indrarti & Azuma, 1998; Tokoh, Takabe, Fujita & Saiki, 1998). Moreover, compared to the conventional static fermentation, agitated fermentation could provide a more controllable environment for BC producers, and could enhance the BC production.

In our previous study (Hu, Catchmark & Demirci, 2020), addition of pullulan, an α (1–6) maltotriose polymer, had been proven to enhance BC production and improve the mechanical properties at various concentrations. To further reduce the production cost, a co-culture fermentation was also implemented. For co-culturing, the BC producer, *Komagataeibacter hansenii*, was inoculated together with a pullulan-producing fungus, *Aureobasidium pullulans*. BC produced in co-culture systems has been examined previously. For instance, symbiotic culture of bacteria and yeast (SCOBY), commonly used to produce fermented tea beverage (Kombucha) is a biofilm containing lactic acid bacteria (mainly *Acetobacter* sp.) and yeast (mainly *Saccharomyces* sp.). SCOBY is mainly composed by BC produced by the lactic acid bacteria, and study has shown that SCOBY could be a potential source of BC products (Jayabalan, Malbaša, Lončar, Vitas & Sathishkumar, 2014; Amarasekara, Wang & Grady, 2020; Villarreal-Soto, Beaufort, Bouajila, Souchard & Taillandier, 2018). However, SCOBY is a symbiotic system of *Acetobacter* sp. and yeast, and there is a limited understanding on the yield and mechanical properties of such co-culture system. Co-culturing BC producer with some fungal strains had been studied (Gromovykh et al., 2018). However, no study in the literature had been conducted prior to our research aiming at improving BC production and mechanical behaviors.

Our previous co-culturing method had produced BC with significantly higher Young's modulus and tensile strength, but the BC production remained similar to the controls. Following the findings, this study was conducted to provide further understanding of co-culture conditions. The goal of this study is to analyze the effect of medium composition on production and the mechanical properties of BC nanocomposite produced in the co-culture fermentation. The hypothesis was that the BC production and mechanical properties could be changed in response to the composition of nutrient sources in the medium. To achieve the goal, this study is undertaken to evaluate the production of BC by using response surface methodology (RSM) and the validation of the local high points in shake-flasks and benchtop bioreactors. This study provides a more in-depth understanding of the behaviors of the co-cultured microorganisms in response to various combinations of nutrient sources.

2. Materials and methods

2.1. Microorganisms and media

Komagataeibacter hansenii (ATCC 23769, previously known as *Gluconacetobacter hansenii* ATCC 23769) was selected as the BC producer since the strain produces negligible amount of exopolysaccharides (minimal free polysaccharides, and approximately 0.2% hard-to-extract exopolysaccharides) besides BC in glucose medium (Fang & Catchmark, 2015). Also, *Aureobasidium pullulans* (ATCC 201253) was selected as pullulan producer based on our previous research (Cheng, Demirci & Catchmark, 2009; Cheng et al., 2009a). The base medium used for co-culturing was a combination of standard glucose-based Hestrin and Schramm (HS) medium for *K. hansenii* (Hestrin & Schramm, 1954) and the base medium for *A. pullulans* growth (Cheng et al., 2009). The medium contains 50 g/L of glucose, 10 g/L of yeast extract, 5 g/L of peptone, 1.2 g/L of citric acid, 2.7 g/L of Na_2HPO_4, 5 g/L of KH_2PO_4, 5 g/L of $(NH_4)_2SO_4$, 1 g/L of NaCl, and 0.5 g/L of $MgSO_4 * 7H_2O$. Both microorganisms were obtained from American Type Culture Collection (ATCC, Manassas, VA) and activated following the ATCC guidelines (ATCC® 23769™ and ATCC® 201253™). The working cultures were maintained at 4 °C and sub-cultured bi-weekly to maintain viability. The stock cultures were stored in 20% glycerol at −80 °C.

For inoculum preparation, *K. hansenii* stock culture was inoculated (1%) in 250-ml flasks that contain 100-ml of the sterile base medium. The inoculated medium was incubated at 30 °C for 3 days. After 3 days, 3% of cellulase solution (Sigma Aldrich, St. Louis, MO) was added to hydrolyze the cellulose produced and release the entrapped cells, and the flasks were then incubated again at 30 °C and agitated at 150 rpm overnight. Then, the broth was centrifuged at 2500 x *g* for 5 min, and the supernatant was decanted to collect cells. The cells were then washed using the sterile fresh medium for 3 times to wash out the remaining cellulase. The washed cells were resuspended in 20 ml of sterile fresh basic medium as the inoculum for the BC fermentation. For *A. pullulans* inoculum, the stock culture was inoculated (1%) in 250-ml flasks that contain 100 ml of sterile basic medium and incubated at 30 °C, 200 rpm for 3 days. The broth was then used directly as the inoculum for the co-culture fermentation.

2.2. Co-culture fermentation in shake-flasks

The inoculum for both of the cultures was inoculated (1% each) in 250-ml flasks containing 100 ml of the medium. After inoculation, the shake-flask fermentations were performed at 30 °C, 200 rpm for 7 days based on Response Surface Methodology (RSM) design. After 7 days of fermentation, the broth was filtered using gauze cloth (Fabric.com, Kennesaw, GA). The collected BC was then submerged into 0.1 M NaOH and put into an 80 °C water bath for 1 day to dissolve all the biomass. After 1 day soaking in NaOH, the BC flocs were filtered again and washed with DI water until the pH was neutralized at pH 7.0 and kept at 4 °C for further analysis.

2.3. Response surface methodology (RSM)

Box-Behnken Response Surface Methodology (RSM) design was used to evaluate different medium compositions. Three significant variables were chosen, specifically glucose as the carbon source and yeast extract and peptone as the nitrogen sources, because these three nutrients are shown to be the most significant parameters for BC and pullulan production (Seo et al., 2004; Son, Heo, Kim, & Lee, 2001). The ranges of the nutrients were chosen based on preliminary experiments: for glucose, the range was 50 - 150 g/L; for yeast extract, the range was 20 - 50 g/L; for peptone, the range was 0–10 g/L. A total of 15 runs were conducted, and the BC productions from these 15 runs were recorded. The response surface was generated using Minitab statistical software (Version 17, Minitab LLC., State College, PA). The detailed experimental design is shown in Table 1. The productions of BC in response to different combinations of these variables were recorded, and 3-D surface plots were generated.

After the generation of the response surface, the local high point on the surface was verified in the shake-flasks and benchtop bioreactors.

2.4. Co-culture fermentation in benchtop bioreactors

Sartorius B-Plus bioreactors (Sartorius Stedim, Göttingen, Germany) with 5-L vessels (4-L working volume) were used. The inoculation was similar to shake-flasks. After inoculation, the fermentations were conducted by using the medium composition at the local high point at 30 °C, 200 rpm, and 1 vvm (4 L/min) of aeration for 7 days. Samples (5–10 ml each) were taken every 24 h for glucose analysis. The initial pH was set at 5, and the pH was not controlled during the fermentation process to simulate the shake-flask conditions.

Table 1
Box-Behnken design for response surface generation*.

Run order	Glucose	Yeast Extract	Peptone
1	+	+	0
2	0	0	0
3	0	+	+
4	–	–	0
5	0	0	0
6	–	0	+
7	+	0	–
8	0	–	–
9	0	–	+
10	+	0	+
11	–	0	–
12	0	+	–
13	–	+	0
14	+	–	0
15	0	0	0

* + represents high end of the selected range (150 g/L of glucose, 50 g/L of yeast extract, and 10 g/L of peptone); - represents the low end of the selected range (50 g/L of glucose, 20 g/L of yeast extract, and 0 g/L of peptone); 0 represents the middle point (100 g/L of glucose, 35 g/L of glucose, and 5 g/L of peptone).

2.5. Analysis

For shake-flasks, the fermentation broth was collected after 7-days of fermentation. For bioreactors, samples were taken every 24 h. Samples were filtered using 0.22-μm syringe filters and then analyzed for BC and glucose.

2.5.1. BC analysis

After the BC flocs were collected and washed, they were shaped into cubes using 1-inch x 1-inch PVC molds and frozen at −80 °C overnight. After freezing, the BC was dried using a freeze-dryer (Freezone 18, Labconco, Kansas City, MO). The freeze-dried BC flocs were then weighed using an analytical balance (Mettler Toledo, Columbus, OH). The BC production (g/L) was determined by dividing the BC weight with the working volume.

2.5.2. Glucose analysis

The concentration of glucose (g/L) was measured using a YSI 2600 Series Biochemistry Analyzer (Xylem Inc., Rye Brook, NY). The analyzer uses enzymes to hydrolyze glucose into gluconolactone and hydrogen peroxide and utilizes linear regression to determine the glucose concentration. The samples taken every 24 h from the bioreactors were used to determine dynamic glucose consumption throughout the fermentation period.

2.5.3. Crystallinity, crystal size, and d-spacing

Crystallinity, crystal size, and d-spacing between crystallized BC planes are useful parameters for determining the effect of pullulan produced by co-culturing on co-crystallization of BC protofibrils. The freeze-dried BC were pressed into a thin layer using an Instron mechanical analyzer (Instron, Boston, MA) with 500 psi of pressure. The pressed BC sheets were then analyzed by x-ray diffraction (XRD) using a PANalytical X'Pert Pro-MPD (Malvern Panalitical Ltd., Malvern, United Kingdom) with Cu Kα radiation generated at 45 mV and 40 mA. The incident beam was emitted from 5° and continued moving until 30° 2θ (Liu & Catchmark, 2018, 2019). The analyzer collected the diffracted x-ray intensity patterns, and the intensity patterns were analyzed using the peak deconvolution method. For deconvolution, PeakFit software (Systat Software Inc., San Jose, CA) was used, and pseudo-Voigt functions were used to integrate the intensity peaks. To evaluate the amorphous cellulose, a peak was added at 21.5° 2θ (Liu & Catchmark, 2019, 2020). The crystallinity index was calculated using the area of the fitted peaks:

$$\text{crystallinity} = \frac{\Sigma\ \text{A(All the peaks without amorphous)}}{\Sigma\ \text{A(All the peaks)}} \quad (1)$$

For evaluating the crystal size on different BC crystal planes, the Scherrer equation was used. The equation depends on the full width half maximum (FWHM) of the integrated peaks:

$$B_{hkl} = \frac{K\lambda}{\sqrt{(\Delta 2\theta)^2 - \left(\Delta 2\theta_{inst}\right)^2}\cos\theta} \quad (2)$$

In the equation, B_{hkl} represents the crystal size at a specific plane, K is the shape factor (related to the method of taking the width of peaks, $0.89 < K < 1$). λ represents the wavelength of X-ray used (1.54059 Å). $\Delta 2\theta$ is FWHM of the peak measured, and $\Delta 2\Delta_{inst}$ is the instrumental width, which is 0.0018 radians for the method used.

The d-spacing between the BC crystalline planes are calculated using Bragg's Law:

$$d = \frac{\lambda}{2\sin\theta} \quad (3)$$

In the equation λ, is the wavelength of the incident beam, and θ represents the scattering angle for the specific plane.

2.5.4. Ribbon width and bundling behavior

Apreo scanning electron microscope (SEM) was used (Thermo Fisher Scientific, Waltham, MA) to visually observe the bundling behavior and measure the BC ribbon width. Freeze-dried BC samples were coated with 10 nm of iridium coating using a sputter coater (EM ACE600, Leica Microsystems, Wetzlar, Germany). After SEM images were taken, 50 fibers on the images were randomly picked, and the widths of the fiber were measured directly. The average BC fiber widths were measured and compared.

2.5.5. Mechanical properties

Three mechanical properties were measured using a dynamic mechanical analyzer, DMA 800 (Texas Instruments, Dallas, TX): Young's modulus, stress, and strain at the yield points. The pressed BC samples were cut into rectangular shapes (2–3 mm width and 10–14 mm length). Before being clamped on the machine, the width and the thickness of the samples were measured using a caliper. After being mounted on tension clamp with 0.05 N preload force, the lengths of the sample between the tension clamps were then measured. The DMA then applied forces on the BC to stretch the sample at a constant rate of 0.25% elongation per minute until the sample broke. During the stretching, stress applied to the cross-sectional area of the sample was calculated automatically by DMA (Eq. (4)), and the strain was also calculated by DMA using ΔL/Lo, where ΔL is the length of elongation, and Lo is the original length of the samples.

$$\text{stress (S)} = \frac{\text{applied force (F)}}{\text{width (W)} * \text{thickness (D)}} \quad (4)$$

Table 2
Nutrient composition and results for the 15 individual runs for the response surface methodology (RSM).

Run order	Glucose%	YE%	Peptone%	BC Dry Weight (g/L)
1	15	5	0.5	0.15
2	10	3.5	0.5	0.193
3	10	5	1	0.305
4	5	2	0.5	0.298
5	10	3.5	0.5	0.25
6	5	3.5	1	0.329
7	15	3.5	0	0.156
8	10	2	0	0.278
9	10	2	1	0.24
10	15	3.5	1	0.18
11	5	3.5	0	0.223
12	10	5	0	0.168
13	5	5	0.5	0.223
14	15	2	0.5	0.17
15	10	3.5	0.5	0.277

After the mechanical data was acquired, stress *vs.* strain was plotted. For BC samples, the region representing elastic deformation appeared at low values of strain, and the slope of this linear region was used as the elastic modulus. Stress and strain at the yield points were recorded as the representation of tensile strength and elongation capability of BC samples.

2.5.6. Statistical analysis

Most of the data collected regarding BC production, Young's modulus, tensile strength, elongation capabilities, BC ribbon width, crystallinity, crystal size, and d-spacing were recorded, represented, and compared using Excel (Microsoft Corporation, Redmond, WA). For BC ribbon width frequency comparison, Minitab statistical software was also used (Version 17, Minitab LLC., State College, PA). The mean values were compared using standard *t*-test ($p < 0.05$) for data collected, and the comparisons were visualized using histograms and dot plots. The error bar represents standard error among the repetitions.

3. Results

3.1. RSM result

The results of the 15 runs for RSM are shown in Table 2. A 3-D response surface plot was produced based on the results (Fig. 1). The ANOVA of this model had been checked and modified (Fig. 1S) so that all the variables had significant influences on the model. The model had an R^2 of 0.9371, the adjusted R^2 was 0.9022, and the predicted R^2 for this model was 0.9030. RSM model is represented by Equation 5.

$$\text{BC production (g/L)} = -18.91-(-11.29 * \text{Glu})-(-4.32*\text{YE})+5.17*\text{Pep} -(-7.56 * \text{Glu} * \text{Glu}) + 7.28 * \text{YE} * \text{Pep} \quad (5)$$

Where, Glu-represents the concentration of glucose in the medium (in %, g/100 ml); YE represents the concentration of yeast extract (%), and Pep represents the concentration of peptone (%).

According to the model, the BC production was the highest with 63 g/L (6.3%) of glucose (Fig. 1(a and b)). The effect of yeast extract and peptone is more complicated: the combination of low concentrations of yeast extract and peptone (low-low) and the combination of high levels of yeast extract and peptone (high-high) resulted in better BC production (Fig. 1(c)).

To verify the model, both the low-low condition and the high-high condition were verified in the shake-flasks ($n = 6$). The detailed culture media composition and the result from the shake-flask are shown in Table 3.

The predicted average BC productions all had large variations (wide 95% CI). The BC produced in the low-low condition was consistent with the result predicted by the model. It had shown a 22.4% increment in BC production for shake-flask co-culture fermentation compared to the original medium (0.249 ± 0.007 g/L). The high-high condition, in contrast, had an even higher variation when predicted by the model, and the actual BC production was lower than the original medium.

Both conditions were also verified in benchtop bioreactors in duplicate runs. For the low-low condition, the BC production in the bioreactors (0.1207 g/L) was only 40% of the shake-flask conditions. For the high-high conditions, the average BC production was consistent with the shake-flask (0.1805 g/L), but a large variation was observed between the two runs.

Due to the complexity of cell behaviors in rich medium (high-high condition), only the BC nanocomposites produced in the low-low condition were further characterized.

3.2. Crystallinity, crystal size, and d-spacing

The XRD intensity patterns for the low-low condition was collected in shake-flasks and bioreactors. For the bioreactors, most (~85%) of the collected BC was attached to the shaft (Fig. 2S). The intensity patterns are shown in Fig. 2.

Three major peaks representing the (100), (010), and (110) crystal planes were detected for all of the conditions. All of the peaks had similar 2θ angles compared to the control. However, for the low-low condition, slightly broader peaks were detected for BC produced in the bioreactor. Crystallinity, crystal size, and the d-spacing are shown in Table 4.

No significant difference in crystallinity of BC was observed for all the conditions. For shake-flasks, the crystal sizes on the (010) and (110) crystalline planes were reduced. BC produced in the bioreactors had lower d-spacings and crystal sizes on the (100), (010) and (110) planes compared to the shake-flask conditions.

3.3. BC ribbon width

The ribbon widths for BC produced are shown in Fig. 3. Increment in average and maximum BC ribbon width was observed for the low-low condition, representing enhanced bundling of BC microfibrils.

3.4. Mechanical properties

When plotting the stress *vs.* strain while the samples deform, all of the samples exhibited linear elastic deformation, followed by long tails of plastic deformation until the samples broke at the highest stress they endure. Therefore, the stress at the break points could be used to represent the tensile strength. The modulus, tensile strength, and elongation were recorded in Fig. 4. The low-low condition produced BC with significantly better tensile strength in shake-flasks and bioreactors compared to BC controls and the co-cultured BC in the original medium. The elastic modules for the low-low condition increased significantly in shake-flasks, but the modules reduced in the bioreactor to a level slightly higher (not significant) than the control and the co-cultured BC in the original medium. The elongation capabilities for all of the samples were similar due to large variances.

3.5. Glucose analysis

The low-low condition had an average glucose consumption of 34.19 ± 0.92 g/L, while the high-high conditions had a glucose consumption of 28.44 ± 2.85 g/L in shake-flasks after 7 days. Both of the condition had similar glucose consumption compared to the control (33.76 ± 1.93 g/L).

The glucose concentration in the bioreactors was measured every 24 h (Fig. 5). For the low-low condition, glucose was spent at the highest rate for the first 24 h. Over 24 h, the glucose consumption rate reduced and maintained at an approximately constant level. Approximately 30 g/L of glucose consumed for both of the conditions after 7 days for both bioreactors.

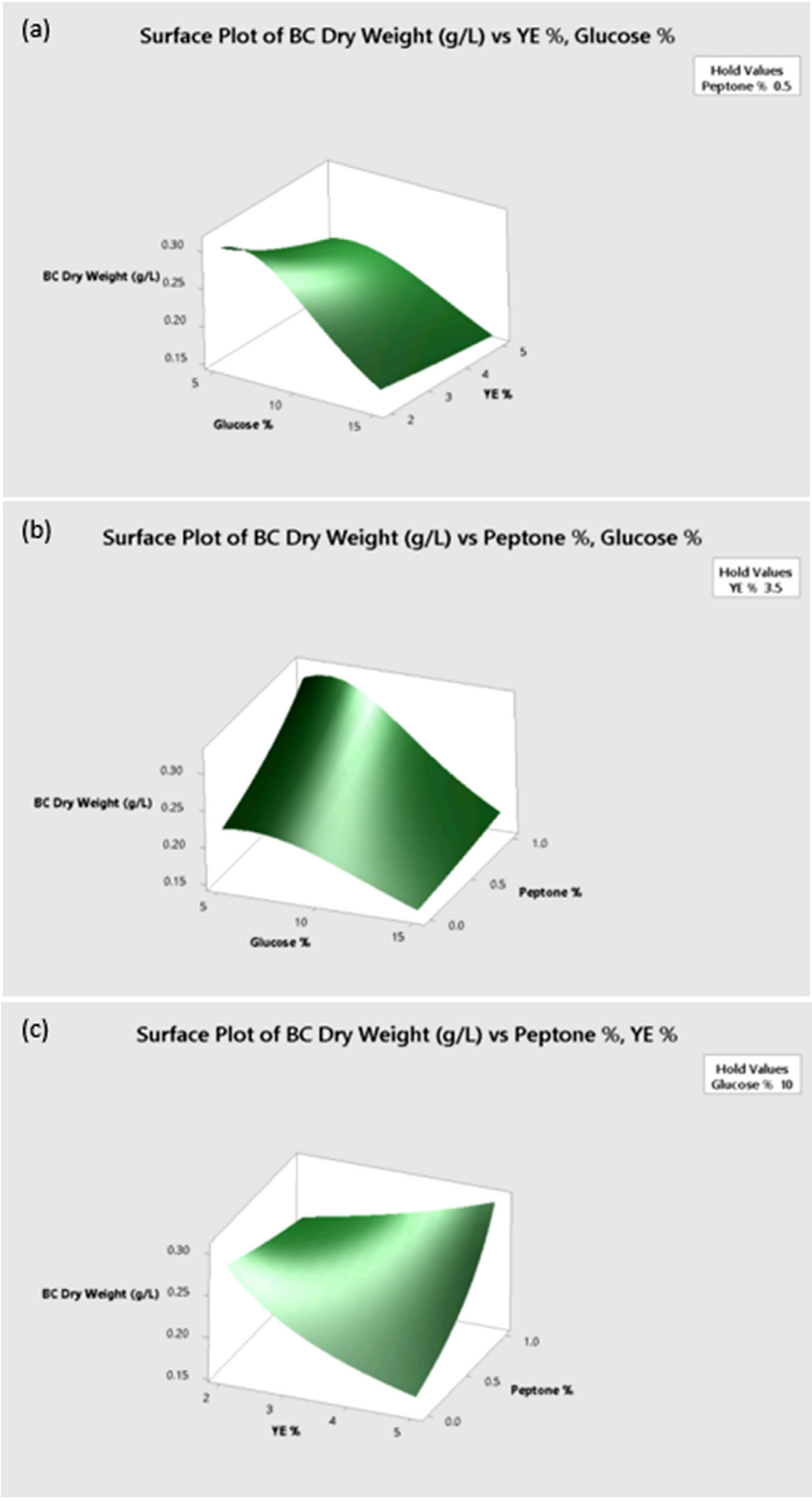

Fig. 1. Response surface of BC production in response to a) glucose and yeast extract; b) glucose and peptone; c) yeast extract and peptone.

4. Discussion

Since most of the polysaccharides affect BC production by altering BC crystallization or the physical formation of BC crystalline, it is essential to understand the mechanism of *K. hansenii* producing BC. After being polymerized and extruded from *K. hansenii* by multi-enzyme cellulose synthase complex, the parallel glucan chains (BC protofibrils) form crystalline BC microfibrils through co-crystallization (Fang & Catchmark, 2012; Lin et al., 2013). BC microfibrils have typical diameters of approximately 3.5 nm (Chinga-Carrasco, 2011), and they form larger

Table 3
Media composition and BC production for the low-low and the high-high conditions co-culturing fermentation in shake-flasks ($n = 6$).

Ingredient	Low-low	High-high
Glucose (g/L)	62.2	62.7
Peptone (g/L)	0	10
Yeast Extract (g/L)	20	50
Citric Acid (g/L)	1.2	1.2
Na_2HPO_4 (g/L)	2.7	2.7
KH_2PO_4 (g/L)	5	5
$(NH_4)_2SO_4$ (g/L)	5	5
NaCl (g/L)	1	1
$MgSO_4 * 7H_2O$ (g/L)	0.5	0.5
Average BC production (95% CI) (g/L)	0.3478 (0.2592, 0.7786)	0.3901 (0.2703, >0.8)
BC production (shake-flask) (g/L)	0.3048 ± 0.02	0.1852 ± 0.01

Table 4
Crystallinity, crystal size, and D-spacing for BC produced in control and the low-low condition ($n = 3$, groups with different letters have significant differences, $p < 0.05$).

	Control	Low-low (shake-flasks)	Low-low (bioreactor)
Crystallinity (%)	81.20 ± 3.24 [a]	85.09 ± 0.82 [a]	78.10 ± 2.55 [a]
d-spacing (Å)			
100	6.08 ± 0.01 [a]	6.04 ± 0.02 [ab]	5.99 ± 0.03 [bc]
010	5.24 ± 0.00 [a]	5.24 ± 0.02 [a]	5.18 ± 0.02 [b]
110	3.90 ± 0.00 [a]	3.90 ± 0.01 [a]	3.88 ± 0.01 [abc]
Crystal size (Å)			
100	52.90 ± 0.41 [a]	52.78 ± 0.28 [a]	49.27 ± 0.52 [c]
010	75.52 ± 4.28 [a]	59.88 ± 0.73 [b]	61.67 ± 2.01 [b]
110	59.33 ± 0.71 [a]	56.80 ± 0.45 [b]	54.86 ± 0.14 [c]

BC ribbons by going through two processes: 1) Physical aggregation, in which BC microfibrils physically interact with each other under the influence of hydrogen bonding or glucan chain interaction; 2) Bundling, in which BC microfibrils aggregate under the influence of polysaccharides. Co-crystallization, physical aggregation, and bundling occur simultaneously during BC formation, but with different degrees (Fang & Catchmark, 2014; Liu & Catchmark, 2018, 2019, 2020). This section discussed the influence of co-culture fermentation on BC formation process, production, and mechanical properties.

4.1. *Effect of co-culture on BC synthesis*

Based on our previous study, it was concluded that in agitated fermentation, the further reduction of BC crystal size in co-culture fermentation was also caused by the pullulan produced by *A. pullulans* (Hu, Catchmark and Demirci, 2020). The reduction of crystal size was consistent with the studies conducted by Atalla (1993), Uhlin (1995), and Botten (2008), in which the addition of xyloglucan, xylan, and mannan had caused a reduction to BC crystal size. It was therefore hypothe-

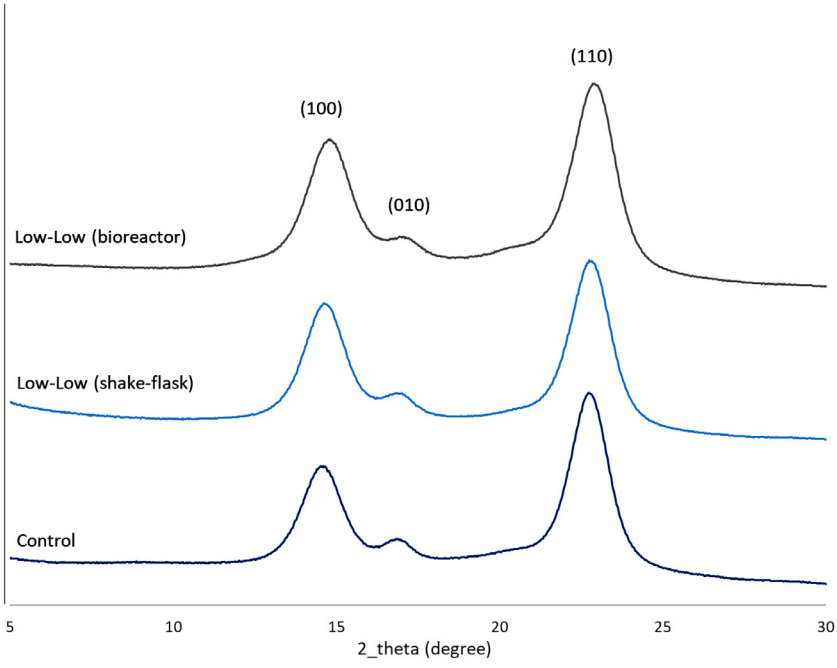

Fig. 2. XRD intensity data collected for shake-flasks and bioreactors under the low-low condition (BC controls in shake-flasks were provided as reference).

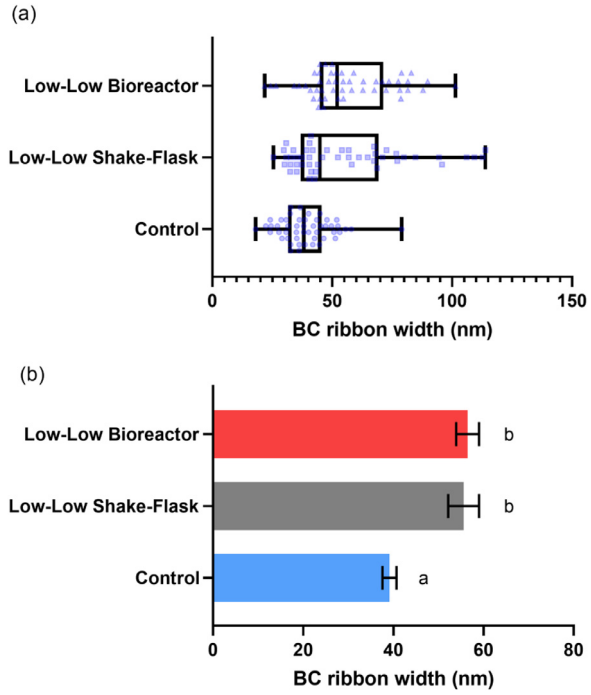

Fig. 3. a). Box-plot for BC ribbon width and b). Comparison of average BC ribbon width (n = 50) (for average ribbon width, groups with different letters have significant differences, $p < 0.05$).

sized that pullulan, due to the existence of α (1–4) and α (1–6) glycosidic bonds, has a preferential affinity to crystallized, ordered BC microfibrils on (010) and (110) planes, and the binding of pullulan on BC protofibrils disrupts co-crystallization, causing a reduced crystal size. Therefore, the low-low conditions resulted in BC with smaller crystal size in shake-flasks.

The change in d-spacing between BC planes and BC crystal size in the bioreactors were also observed in other studies. According to Czaja, Romanovicz and Brown (2004), reduced BC crystal sizes on the (010) and (110) planes were found and shifts of d-spacing on (100) and (110) planes were also observed. The study concluded that the high shear stress generated by agitation had interfered with the co-crystallization of nascent BC protofibrils, making them more favorable to form smaller microfibrils. Moreover, the study had also proven the high shear stress could increase the proportion of cellulose I_β, a more stable allomorph, thus reducing the d-spacing between BC planes (Czaja, Romanovicz & Brown, 2004). The hypothesis was also consistent with the findings of studies conducted by Yamamoto, Horii and Hirai (1996)) and Hirai, Tsuji, Yamamoto and Horii (1998). Therefore, in this study, it was hypothesized that compared to shake-flasks, bioreactor produced more shear stress by its propeller. The increased shear stress made uncrystallized BC protofibrils more favorable in forming smaller BC microfibrils and increased the production of more stable cellulose I_β. Therefore, BC with reduced crystal size and smaller d-spacing was produced in the bioreactor.

4.2. Effect of the co-culture on BC production

The low-low condition resulted in enhanced BC production compared to the original co-culture fermentation. We hypothesize that the improved BC production in the low-low condition is because pullulan disrupted co-crystallization of BC microfibrils, which was proven to be the rate-limiting step for BC production (Benziman, Haigler, Brown, White, & Cooper, 1980). A similar increment in BC production was observed in the research conducted by Cheng et al. (2011) with carboxymethyl cellulose (CMC) added during the fermentation, and the

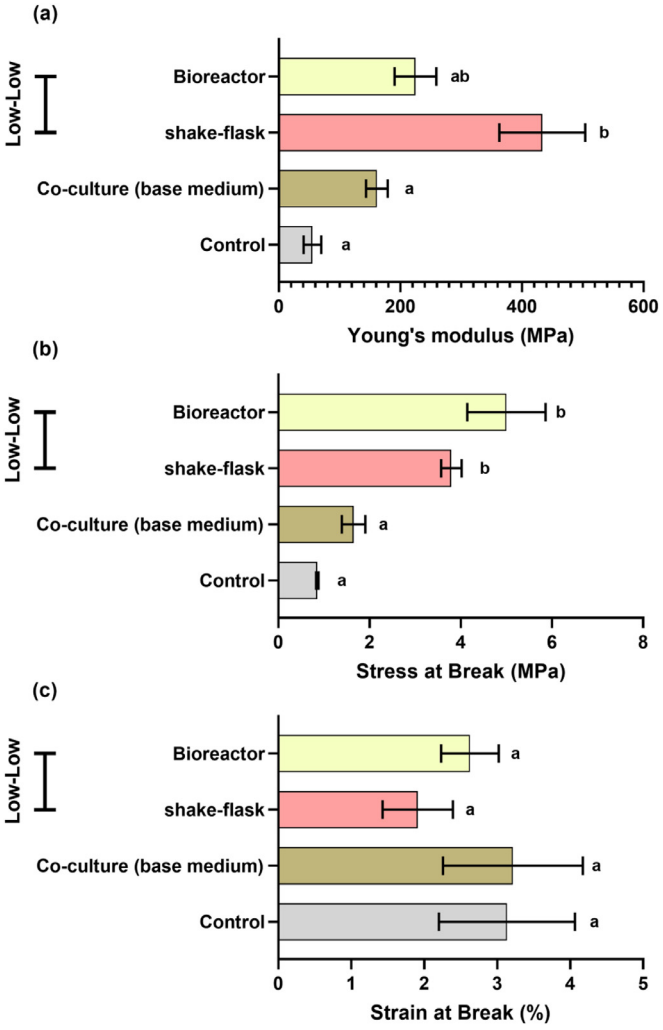

Fig. 4. a) Young's modulus, b) tensile strength, and c) strain at the breaking points for BC controls and BC produced in the low-low condition (n = 3, groups with different letters have significant differences, $p < 0.05$).

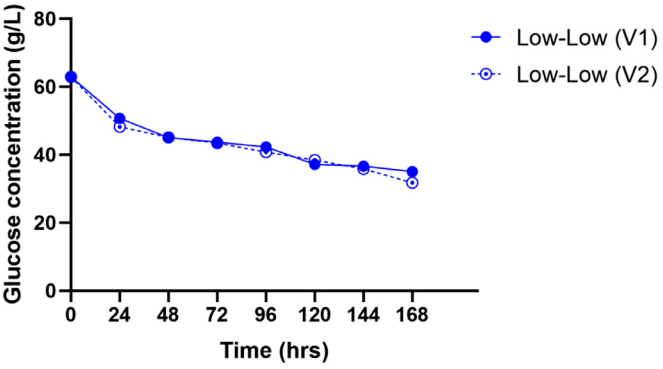

Fig. 5. Glucose concentration in the bioreactors for the low-low condition during the 7-day fermentation (duplicated, V1 and V2 represent each individual run under the same condition).

reduced crystal size (Table 4) supports the hypothesis of disrupted co-crystallization. However, in the richer high-high medium, an increased concentration in nitrogen source could improve the growth of *A. pullulans*, leading a more severe competition between the microorganisms inoculated, thus further limiting the growth and BC production of *K. hansenii*. Forms of competition include but not limited to competition

on other minor nutrients (salts, minerals), oxygen depletion, or direct interaction between the cells (Goers, Freemont & Polizzi, 2014). For instance, various studies had defined *A. pullulans* as an active competitor on different nutrients and space (Agirman & Erten, 2020; Bozoudi & Tsaltas, 2018; Di Francesco et al., 2020).

In the bioreactors, the BC productions were significantly lower than shake-flasks in the low-low condition. A possible explanation is that in bioreactors, the fermentation conditions (better nutrient distribution and aeration) were more favored by *A. pullulans* than by *K. hansenii*. Another possible explanation of a lower BC production in the bioreactors is the shear stress. The studies conducted by other researchers (Chao, Mitarai, Sugano & Shoda, 2001; Ishida, Mitarai, Sugano & Shoda, 2003; Cheng et al., 2011) had shown that agitated fermentation could generate harmful shear stress that lower the BC production. It was also proven that bioreactors generate higher shear force against *K. hansenii* compared to shake-flasks (Chao, Mitarai, Sugano, & Shoda, 2001; Ishida, Mitarai, Sugano, & Shoda, 2003). Therefore, the BC production was significantly lower for the low-low condition in the bioreactors compared to shake-flasks. Alternative reactor designs could be considered for future co-culture studies. For instance, Cheng et al. (2009, 2011) had shown that plastic composite support (PCS) biofilm bioreactors could improve BC and pullulan production of *K. hansenii* and *A. pullulans* by improving the biomass attachment.

4.3. Effect of the co-culture on BC mechanical properties

For BC produced in shake-flasks, Young's moduli and tensile strength were also increased significantly compared to the control. For the bioreactors, under the low-low condition, suspended BC had slightly higher Young's modulus, tensile strength, and elongation capability compared to those cultivated in shake-flasks, but the attached BC had slightly reduced Young's modulus, while the stress at the point of break and elongation capabilities were similar to the shake-flasks.

In our previous study (Hu, Catchmark and Demirci, 2020), BC produced by *K. hansenii* inoculated in the base medium containing 0.36, 1, 1.5, and 2% of pullulan, as well as the co-cultured BC, were tested. The previous study has shown a significantly better BC mechanical property when cultivated in the medium with 1% pullulan addition and by co-culturing (Hu, Catchmark and Demirci, 2020). The observations in this study were similar to our previous study with 1% of pullulan addition. The mechanism pullulan enhancing the BC mechanical properties in shake-flasks was discussed in our previous study: pullulan has a high affinity to BC protofibrils and microfibrils (Section 4.1). With the pullulan production in the low-low condition, the BC microfibrils were brought closer to each other, forming a more reticulated structure with more hydrogen bonding between the microfibrils. According to Liu and Catchmark (2019, 2020), more hydrogen bonds would lead to a better mechanical property since the main interactional force contributing to the BC mechanical properties is the number of hydrogen bonds between BC microfibrils.

For the bioreactors, it was hypothesized that the shift in mechanical properties was caused by a mixed effect of pullulan and agitation. In the bioreactor, the pullulan production was enhanced, due to a possibly improved cell growth. Since the mechanical property of BC has a positive relationship with pullulan concentration at 0–1% (Hu, Catchmark and Demirci, 2020), increased production of pullulan improved the tensile strength of BC in the bioreactor for the low-low condition.

In contrast to the tensile strength, the Young's modulus of BC was reduced in the bioreactors. Similar behavior was observed in the study conducted by Cheng et al. (2009a), in which a biofilm reactor was used for BC fermentation. It was concluded in the study that bioreactors could produce higher agitation, reducing the degree of polymerization of BC, thus lowering Young's modulus (Cheng et al., 2009a). Therefore, it was hypothesized that since most of the BC in the bioreactor was formed on or close to the propeller shaft, where significantly higher shear stress was generated, the attached BC had a slightly reduced elastic modulus although the tensile strength of BC was significantly higher due to the existence of pullulan.

5. Conclusions

The RSM result had shown that the low-low condition helped increase the BC production while enhanced the mechanical properties compared to the original co-culture fermentation. However, other factors affecting the growth of *K. hansenii* might have occurred during the co-culture fermentation, making the high-high condition not behaving as predicted by the RSM model, but the improved BC production in the low-low condition indicated that the co-culture fermentation can be affected by medium composition.

This study had also proven that co-culture fermentation in the bioreactors could maintain the mechanical properties of BC compared to the shake-flasks. However, the BC production in the bioreactors was reduced significantly, possibly due to competition on nutrients and space between *K. hansenii* and *A. pullulans*. The study had shown that pullulan produced by the co-culture fermentation could bind to both ordered BC microfibrils and disordered BC protofibrils, altering bundling behavior and physical aggregation of BC microfibrils. Although the BC production was low, the fermentation still has the potential to be further optimized and has value since the co-culture fermentation could produce BC with a significantly better mechanical property. Moreover, the BC producer (ATCC 23769) was selected because this strain produces a negligible amount of EPS, which could introduce uncertainty to the result. However, there are other BC producers with a better production rate (Cheng, Catchmark & Demirci, 2009b; Fang & Catchmark, 2015). Since pullulan could affect the formation of BC, this co-culturing method has the potential to be applied to more efficient BC producers.

Overall, this study had supported the hypothesis that the BC production and mechanical property can be changed in response to co-culture medium composition. More in-depth studies on the interaction and competition between the inoculated microorganisms are needed, but we believe that the co-culturing method has the potential to produce BC products with better properties. This research is a preliminary step toward future optimization and scale-up studies before commercializing the co-culture BC fermentation process. Possible optimization parameter to consider in the future include the concentrations of salts (such as ammonium sulfate), different bioreactor designs, and the degree of contact between the two microorganisms inoculated.

Declaration of Competing Interest

None.

Acknowledgments

This work was in-part supported by the USDA National Institute of Food and Agriculture Federal Appropriations under Project PAES 4602 [grant number 1009850] and Penn State Center of Excellence in Industrial Biotechnology (CoEIB) IMPACT SEED Grant.

Supplementary materials

Supplementary material associated with this article can be found, in the online version, at doi:10.1016/j.carpta.2020.100028.

References

Agirman, B., & Erten, H. (2020). Biocontrol ability and action mechanisms of *aureobasidium pullulans* GE17 and *meyerozyma guilliermondii* KL3 against *penicillium digitatum* DSM2750 and *penicillium expansum* DSM62841 causing postharvest diseases. *Yeast (Chichester, England), 2020*, 1–12.

Amarasekara, A. S., Wang, D., & Grady, T. L. (2020). A comparison of kombucha SCOBY bacterial cellulose purification methods. *SN Applied Sciences, 2*(2) Article 240.

Amnuaikit, T., Chusuit, T., Raknam, P., & Boonme, P. (2011). Effects of a cellulose mask synthesized by a bacterium on facial skin characteristics and user satisfaction. *Medical Devices: Evidence and Research, 4*(1), 77–81.

Backdahl, H., Helenius, G., Bodin, A., Nannmark, U., Johansson, B. R., Risberg, B., et al. (2006). Mechanical properties of bacterial cellulose and interactions with smooth muscle cells. *Biomaterials, 27*(9), 2141–2149.

Benziman, M., Haigler, C. H, Brown, R. M., White, R., & Cooper, K. M (1980). Cellulose biogenesis: Polymerization and crystallization are coupled processes in *Acetobacter xylinum*. *Proceedings of the National Academy of Sciences of the United States of America, 77*(11), 6678–6682.

Bozoudi, D., & Tsaltas, D. (2018). The multiple and versatile roles of *Aureobasidium pullulans* in the vitivinicultural sector. *Fermentation, 4*, 85–99.

Chao, Y., Mitarai, M., Sugano, Y., & Shoda, M. (2001). Effect of addition of water-soluble polysaccharides on bacterial cellulose production in a 50-L airlift reactor. *Biotechnology Progress, 17*(4), 781–785.

Cheng, K. C., Catchmark, J. M., & Demirci, A. (2009b). Enhanced production of bacterial cellulose by using a biofilm reactor and its material property analysis. *Journal of Biological Engineering, 3*(1), 12.

Cheng, K. C., Catchmark, J. M., & Demirci, A. (2011). Effects of CMC addition on bacterial cellulose production in a biofilm reactor and its paper sheets analysis. *Biomacromolecules, 12*(3), 730–736.

Cheng, K. C., Demirci, A., & Catchmark, J. M. (2009). Effects of plastic composite support and pH profiles on pullulan production in a biofilm reactor. *Applied Microbiology and Biotechnology, 86*(3), 853–861.

Cheng, K., Catchmark, J. M., & Demirci, A. (2009a). Effect of different additives on bacterial cellulose production by *Acetobacter xylinum* and analysis of material property. *Cellulose (London, England), 16*, 1033–1045.

Chi, K., & Catchmark, J. M. (2017). The influences of added polysaccharides on the properties of bacterial crystalline nanocellulose. *Nanoscale, 9*(39), 15144–15158.

Chinga-Carrasco, G. (2011). Cellulose fibres, nanofibrils and microfibrils: The morphological sequence of MFC components from a plant physiology and fibre technology point of view. *Nanoscale research letters, 6*, 417–423.

Çoban, E. P., & Biyik, H. (2011). Evaluation of different pH and temperatures for bacterial cellulose production in HS (Hestrin-Scharmm) medium and beet molasses medium. *African Journal of Microbiology Research, 5*(9), 1037–1045.

Czaja, W., Romanovicz, D., & Brown, R. M. (2004). Structural investigations of microbial cellulose produced in stationary and agitated culture. *Cellulose (London, England), 11*(3/4), 403–411.

Di Francesco, A., Di Foggia, M., Corbetta, M., Baldo, D., Ratti, C., & Baraldi, E. (2020). Biocontrol activity and plant growth promotion exerted by *Aureobasidium pullulans* strains. *Journal of Plant Growth Regulation*. https://doi.org/10.1007/s00344-020-10184-3.

Fang, L., & Catchmark, J. M. (2012). Analysis of *Gluconacetobacter xylinus* exopolysaccharides and its impacts on bacterial cellulose production and crystallization. In *Proceedings of the American society of agricultural and biological engineers annual international meeting (ASABE)*.

Fang, L., & Catchmark, J. M. (2014). Characterization of water-soluble exopolysaccharides from Gluconacetobacter xylinus and their impacts on bacterial cellulose crystallization and ribbon assembly. *Cellulose (London, England), 21*, 3965–3978.

Fang, L., & Catchmark, J. M. (2015). Characterization of cellulose and other exopolysaccharides produced from *Gluconacetobacter strains*. *Carbohydrate Polymers, 115*, 663–669.

Goers, L., Freemont, P., & Polizzi, K. M. (2014). Co-culture systems and technologies: Taking synthetic biology to the next level. *Journal of the Royal Society Interface, 11*(96) 20140065.

Gromovykh, T. I., Gavryushina, I. A., Sadykova, V. S., Feldman, N. B., Dmitrenok, A. S., & Ayrapetova, A. Y. (2018). Obtaining immobilized mycelium of basidiomycete fomitopsis officinalis (Vill.:FR.) bond. et sing., producer of agaricic acid. *Antibiotics and Chemotherapy, 63*(9–10), 3–9 (In Russ.).

Gullo, M., China, S. L., Petroni, G., Gregorio, S. D., & Giudici, P. (2019). Exploring K2G30 genome: A high bacterial cellulose producing strain in glucose and mannitol based media. *Frontiers in Microbiology, 10* Article 58.

Gullo, M., Sola, A., Zanichelli, G., Montorsi, M., Messori, M., & Giudici, P. (2017). Increased production of bacterial cellulose as starting point for scaled-up applications. *Applied Microbiology and Biotechnology, 101*(22), 8115–8127.

Hestrin, S., & Schramm, M. (1954). Synthesis of cellulose by *Acetobacter xylinum*. 2. Preparation of freeze-dried cells capable of polymerizing glucose to cellulose. *Biochemical Journal, 58*(2), 345–352.

Hirai, A., Tsuji, M., Yamamoto, H., & Horii, F. (1998). *In Situ* crystallization of bacterial cellulose III. Influences of different polymeric additives on the formation of microfibrils as revealed by transmission electron microscopy. *Cellulose (London, England), 5*, 201–213.

Hsieh, Y. C., Yano, H., Nogi, M., & Eichhorn, S. J. (2008). An estimation of the Young's modulus of bacterial cellulose filaments. *Cellulose (London, England), 15*(4), 507–513.

Hu, H., Catchmark, J.M., .& Demirci, A. (2020). Effects of pullulan additive and co-culture of *Aureobasidium pullulans* on the production of bacterial cellulose nanocomposite produced by *Gluconacetobacter hansenii* in shake-flasks. Submitted.

Ishida, T., Mitarai, M., Sugano, Y., & Shoda, M. (2003). Role of water-soluble polysaccharides in bacterial cellulose production. *Biotechnology and Bioengineering, 83*(4), 474–478.

Iwata, T., Indrarti, L., & Azuma, J. I. (1998). Affinity of hemicellulose for cellulose produced by *Acetobacter xylinum*. *Cellulose (London, England), 5*, 215–228.

Jagannath, A., Kalaiselvan, A., Manjunatha, S. S., Raju, P. S., & Bawa, A. S. (2008). The effect of pH, sucrose and ammonium sulphate concentrations on the production of bacterial cellulose (*Nata-de-coco*) by *Acetobacter xylinum*. *World Journal of Microbiology and Biotechnology, 24*(11), 2593–2599.

Jayabalan, R., Malbaša, R. V., Lončar, E. S., Vitas, J. S., & Sathishkumar, M. (2014). A review on Kombucha tea—Microbiology, composition, fermentation, beneficial effects, toxicity, and tea fungus. *Comprehensive Reviews in Food Science and Food Safety, 13*, 538–550.

Klemm, D., Ahrem, H., Kramer, F., Fried, W., Wippermann, J., & Kinne, R. W. (2016). Bacterial nanocellulose hydrogels designed as bioartificial medical implants. *Bacterial NanoCellulose: A Sophisticated Multifunctional Material*, 176–198.

Kuo, C., Chen, J., Liou, B., & Lee, C. (2016). Utilization of acetate buffer to improve bacterial cellulose production by *Gluconacetobacter xylinus*. *Food Hydrocolloids, 53*, 98–103.

Lin, S. P., Loira-Calvar, I., Catchmark, J. M., Liu, J. R., Demirci, A., & Cheng, K. C. (2013). Biosynthesis, production and applications of bacterial cellulose. *Cellulose (London, England), 20*(5), 2191–2219.

Liu, K., & Catchmark, J. M. (2018). Effects of exopolysaccharides from *Escherichia coli* ATCC 35860 on the mechanical properties of bacterial cellulose nanocomposites. *Cellulose (London, England), 25*(4), 2273–2287.

Liu, K., & Catchmark, J. M. (2019). Enhanced mechanical properties of bacterial cellulose nanocomposites produced by co-culturing *Gluconacetobacter hansenii* and *Escherichia coli* under static conditions. *Carbohydrate Polymers, 219*, 12–20.

Liu, K., & Catchmark, J. M. (2020). Bacterial cellulose/hyaluronic acid nanocomposites production through co-culturing Gluconacetobacter hansenii and *Lactococcus lactis* under different initial pH values of fermentation media. *Cellulose (London, England), 27*, 2529–2540.

Muangman, P., Opasanon, S., Suwanchot, S., & Thangthed, O. (2011). Efficiency of microbial cellulose dressing in partial-thickness burn wounds. *Journal of the American College of Certified Wound Specialists, 3*(1), 16–19.

Nakagaito, A. N., Iwamoto, S., & Yano, H. (2005). Bacterial cellulose: The ultimate nanoscalar cellulose morphology for the production of high-strength composites. *Applied Physics A: Materials Science and Processing, 80*(1), 93–97.

Nimeskern, L., Martínez Ávila, H., Sundberg, J., Gatenholm, P., Müller, R., & Stok, K. S. (2013). Mechanical evaluation of bacterial nanocellulose as an implant material for ear cartilage replacement. *Journal of the Mechanical Behavior of Biomedical Materials, 22*, 12–21.

Okiyama, A., Motoki, M., & Yamanaka, S. (1992). Bacterial cellulose II. Processing of the gelatinous cellulose for food materials. *Topics in Catalysis, 6*(5), 479–487.

Okiyama, A., Motoki, M., & Yamanaka, S. (1993). Bacterial cellulose IV. Application to processed foods. *Topics in Catalysis, 6*(6), 503–511.

Ross, P., Mayer, R., & Benziman, M. (1991). Cellulose biosynthesis and function in bacteria. *Microbiological Reviews, 55*(1), 35–58.

Seo, H. P., Chung, H. C., Sung, K. K., Richard, A. G., David, L. K., & Jin, W. L. (2004). Mass production of pullulan with optimized concentrations of carbon and nitrogen sources by *Aureobasidium pullulans* HP-2001 in a 100-L bioreactor with the inner pressure. *Journal of Microbiology and Biotechnology, 14*(2), 237–242.

Son, H. J., Heo, M. S., Kim, Y. G., & Lee, S. J. (2001). Optimization of fermentation conditions for the production of bacterial cellulose by a newly isolated *Acetobacter* sp. A9 in shaking cultures. *Biotechnology and Applied Biochemistry, 33*(1), 1–5.

Tokoh, C., Takabe, K., Fujita, M., & Saiki, H. (1998). Cellulose synthesized by *Acetobacter xylinum* in the presence of acetyl glucomannan. *Cellulose (London, England), 5*, 249–261.

Toyosaki, H., Naritomi, T., Seto, A., Matsuoka, M., Tsuchida, T., & Yoshinaga, F. (1995). Screening of bacterial cellulose-producing *Acetobacter* strains suitable for agitated culture. *Bioscience, Biotechnology, and Biochemistry, 59*(8), 1498–1502.

Vazquez, A., Foresti, M. L., Cerrutti, P., & Galvagno, M. (2012). Bacterial cellulose from simple and low cost production media by *Gluconacetobacter xylinus*. *Journal of Polymers and the Environment, 21*(2), 545–554.

Velásquez-Riaño, M., & Bojacá, V. (2017). Production of bacterial cellulose from alternative low-cost substrates. *Cellulose (London, England), 24*(7), 2677–2698.

Villarreal-Soto, S. A., Beaufort, S., Bouajila, J., Souchard, J., & Taillandier, P. (2018). Understanding Kombucha tea fermentation: A review. *Journal of Food Science, 83*(3), 580–588.

Wippermann, J., Schumann, D., Klemm, D., Kosmehl, H., Salehi-Gelani, S., & Wahlers, T. (2009). Preliminary results of small arterial substitute performed with a new cylindrical biomaterial composed of bacterial cellulose. *European Journal of Vascular and Endovascular Surgery, 37*(5), 592–596.

Yamamoto, H., Horii, F., & Hirai, A. (1996). *In situ* crystallization of bacterial cellulose II. Influences of different polymeric additives on the formation of celluloses I_α and I_β at the early stage of incubation. *Cellulose (London, England), 3*(1), 229–242.

Zhao, H., Xia, J., Wang, J., Yan, X., Wang, C., Lei, T., et al. (2018). Production of bacterial cellulose using polysaccharide fermentation wastewater as inexpensive nutrient sources. *Biotechnology & Biotechnological Equipment, 32*(2), 350–356.